Journal of Earthquake Engineering
Publication details, including instructions for authors and subscription information:
http://www.tandfonline.com/loi/ueqe20

Comparison of Nonlinear Static Methods for the Seismic Assessment of Plan Irregular Frame Buildings with Non Seismic Details

Carlos Bhatt [a] & Rita Bento [a]

[a] Instituto Superior Técnico, Technical University of Lisbon, Lisbon, Portugal

Version of record first published: 28 Dec 2011.

To cite this article: Carlos Bhatt & Rita Bento (2012): Comparison of Nonlinear Static Methods for the Seismic Assessment of Plan Irregular Frame Buildings with Non Seismic Details, Journal of Earthquake Engineering, 16:1, 15-39

To link to this article: http://dx.doi.org/10.1080/13632469.2011.586085

Journal of Earthquake Engineering, 16:15–39, 2012

ISSN: 1363-2469 print / 1559-808X online
DOI: 10.1080/13632469.2011.586085

Taylor & Francis
Taylor & Francis Group

Comparison of Nonlinear Static Methods for the Seismic Assessment of Plan Irregular Frame Buildings with Non Seismic Details

CARLOS BHATT and RITA BENTO

Instituto Superior Técnico, Technical University of Lisbon, Lisbon, Portugal

The use of Nonlinear Static Procedures (NSPs) for the seismic assessment of plan irregular buildings is challenging. The most common pushover-based approaches have led to adequate results in regular buildings, and hence, there is a need to verify the validity of such methods on the assessment of irregular structures. In this article, four commonly used nonlinear static procedures (CSM, N2, MPA, ACSM) are applied on the assessment of two existing five- and eight-story plan-asymmetric buildings in Turkey. The accuracy of the different NSPs is evaluated through comparisons with the results derived from nonlinear dynamic analyses. The results are presented in terms of interstory drifts, normalized top displacements, lateral displacement profiles, chord rotations, base shear, and top displacement ratios. The performance of such procedures in evaluating the damage limitation according to the Eurocode8 is also verified. Special attention is given to the ACSM (Adaptive Capacity Spectrum Method) whose performance in 3D plan irregular buildings has recently been tested. Conclusions about the performance of each NSP are outlined at the end of the article.

Keywords Seismic Assessment; Pushover; Nonlinear Static Procedures; Real Existing Plan Irregular Buildings; Torsion

1. Introduction

The nonlinear static procedures (NSPs) are deemed to be very practical tools for assessing the nonlinear seismic performance of structures. On the other hand, the nonlinear dynamic time-history analyses are very time consuming, which is a relevant drawback in design offices, where the deadlines are restrictive. Nowadays, the good performance of NSPs on bridges and planar frames is generally recognized. However, the use of such methods in the case of real existing plan irregular structures has so far been studied by only a limited number of authors, e.g., Chopra and Goel [2004], Fajfar *et al.* [2005], and Bento *et al.* [2010]. This fact limits the ability of NSPs to assess current existing structures, the majority of which are irregular in plan.

The existing studies about this topic usually focus on the evaluation of a single NSP. In order to get useful elements of comparison between different methodologies, the performance of four commonly employed nonlinear static procedures (CSM, N2, MPA, and ACSM) is evaluated in this article. The case studies chosen are two real Turkish RC five- and eight- story buildings with irregularities in plan. Comparison of the results obtained

Received 24 October 2010; accepted 03 May 2011.

Address correspondence to Carlos Bhatt, Department of Civil Engineering and Architecture, Instituto Superior Técnico, Technical University of Lisbon, Av. Rovisco Pais, 1049-001, Lisbon, Portugal; E-mail: cbhatt@civil.ist.utl.pt

with nonlinear dynamic analysis, through the use of semi-artificial ground motions, enables the evaluation of the accuracy of the different NSPs.

In Bento *et al.* [2010], the same NSPs herein analyzed were used to assess the three-story SPEAR building. This article intends to continue the previous study, using more examples of real existing plan-irregular buildings, in order to reach more consolidated conclusions about the use of NSPs in these kinds of structures. The buildings selected to resume this study are quite different from the one already tested, namely in terms of height (number of stories), plan configuration, material properties, and reinforcement details. Additionally, the structural specificities of the eight-story building allow the evaluation of the NSPs performance in these situations.

2. Considered Nonlinear Static Procedures

The nonlinear static procedures discussed in this work can be divided into two groups. The first group contemplates the so-called Capacity Spectrum Method (CSM)—first introduced by Freeman *et al.* [1975] and Freeman [1998], and later included in ATC-40 guidelines [ATC, 1996]—and the N2 method suggested by Fajfar and and Fishinger [1988] and Fajfar [2000] and proposed in Eurocode8 [CEN, 2004]. Each one of these two methods was tested in two variants: CSM-ATC40/CSM-FEMA440 and N2/extended N2. The CSM-FEMA440 considers innovative features given in the FEMA-440 report [ATC, 2005], and the extended N2 method [Fajfar *et al.*, 2005] is an extension of the original N2 to the 3D case.

The second group consists of the recent proposals of Chopra and Goel [2002, 2004] on a Modal Pushover Analysis (MPA) and Casarotti and Pinho [2007], by means of Adaptive Capacity Spectrum Method (ACSM). The last method was only applied once in a 3D plan-asymmetric building [Bento *et al.*, 2010], so one of the aims of this article is to evaluate its performance in other buildings with such kinds of irregularities.

A preliminary comparison between the N2 and the extended N2 method, and the CSM-ATC40 and CSM-FEMA440, was made in terms of story drifts, normalized top displacements, lateral displacement profiles, and chord rotations. The obtained results showed that the Extended N2 procedure led to better results than its original version and that the CSM-FEMA440 proved to be a much improved version with respect to its CSM-ATC40 predecessor [Bento *et al.*, 2010]. Based on this, the Extended N2 method and the CSM-FEMA440 were chosen to be used in the subsequent plots.

The pushover analysis is used in design offices or by researchers to verify the structural performance of newly designed and existing buildings. Therefore, the results obtained with these methods should, first of all, be conservative with respect to the time-history analysis, in order to never underestimate the structural response of the buildings under analysis. The performance of a specific NSP increases if its results get close to the time-history median values, but always conservatively. In this article, the NSPs are evaluated, taking into account these two main characteristics: conservative results and accuracy in respect to the median time-history results.

The different features of the analyzed NSPs are herein described and compared.

2.1. Pushover Analysis Load Pattern

The ACSM uses an adaptive displacement pushover, the so-called DAP [Antoniou and Pinho, 2004]. This type of pushover is fully adaptive in the sense that it incrementally updates the lateral displacement pattern based on the modal properties of the structure at each analysis step. Therefore, it takes into account the stiffness degradation, period

elongation, and progressive structural damage. At each step, the eigenvalues and modes of vibration of the building are calculated considering the current structural stiffness state. The load pattern to be applied in the next step is obtained by doing a combination of these different mode shapes. Therefore, the higher mode effects are taken into account. The spectral shape, that represents the contribution of each period and mode of vibration into the final displacement profile at each analysis step, for a given hazard, is considered through the use of spectral scaling.

The extended N2 method uses a conventional non adaptive force-based pushover. Any reasonable distribution of lateral loads can be used in the N2 method. According to Fajfar [2000], the range of reasonable assumptions is relatively limited, and different assumptions lead to similar results. The Eurocode8 recommends the use of at least two distributions: a first mode proportional load pattern and a uniform load pattern.

The CSM-FEMA440 also advocates a force-based non adaptive conventional pushover, using a first-mode proportional load pattern.

The MPA considers non adaptive force-based pushover analyses based on modal proportional load patterns. It is a multi-run method, using in each run a different load pattern proportional to each mode of vibration of the structure. The final results are obtained by combining the results computed from each pushover curve. Therefore, the method takes into account the higher mode effects.

2.2. MDOF to SDOF Transformation

Instead of using a single control node like the other NSPs, the ACSM computes the equivalent SDOF structural displacement built on the current deformed pattern, which can turn very useful in the 3D case:

$$\Delta_{sys,k} = \frac{\sum_i m_i \Delta_{i,k}^2}{\sum_i m_i \Delta_{i,k}} \tag{2.1}$$

$$M_{sys,k} = \frac{\sum_i m_i \Delta_{i,k}}{\Delta_{sys,k}} \tag{2.2}$$

$$S_{a-cap,k} = \frac{V_{b,k}}{M_{sys,k} g}, \tag{2.3}$$

where
$\Delta_{sys,k}$ - is the SDOF displacement at step k of the pushover analysis;
m_i - is the mass of structural node i;
$\Delta_{i,k}$ - is the displacement of structural node i;
$M_{sys,k}$ - is the equivalent SDOF mass at step k;
$V_{b,k}$ - is the structural base shear at step k;
$S_{a-cap,k}$ - is the SDOF acceleration at step k;
g - is 9.81ms^{-2}.

The other NSPs consider a single control node for the SDOF characterization, usually the center of mass of the roof. In the N2 method, both displacements and the forces of the MDOF are multiplied with the same Gama factor that depends on the mass of each story, the modal displacement at each floor normalized to the roof's center of mass, and of the equivalent mass, in order to obtain the SDOF curve force vs. displacement. The CSM-FEMA440 uses two different coefficients for the transformation of displacements and the

accelerations, in order to calculate the SDOF curve in terms of acceleration vs. displacement. Note that if one divides the SDOF forces in the N2 method by the equivalent mass (as defined by the method) in order to get the SDOF curve acceleration vs. displacement, the equation of the SDOF accelerations will be the same of as the one presented by FEMA 440. The equations of the SDOF displacement transformation are the same in Eurocode 8 and in FEMA 440.

Note that the CSM-FEMA440 and the extended N2 methods use the first mode of vibration in each direction to compute the transformation factor. The MPA uses a different transformation factor for each pushover curve obtained from the corresponding mode of vibration.

2.3. Computation of the Target Displacement

The extended N2 method calculates the SDOF equivalent period from the bilinearization of the SDOF capacity curve and then it uses an inelastic spectrum to compute the target displacement. The method considers the equal displacement rule, which may lead to overestimations of the results. The target displacement chosen is the higher value obtained from the two pushover curves computed with a modal proportional and uniform load patterns.

The computation of the target displacement of the MPA was made in a similar way to the N2 method. However, this method calculates a target displacement for each pushover curve associated to each mode of vibration.

The CSM and the ACSM compute the target displacement by intersecting the SDOF capacity curve with a reduced ADRS (acceleration-displacement response spectrum). The ACSM uses a damping based reduction factor proposed by Lin and Chang [2003], where the damping is computed using the formula proposed by Gulkan and Sozen [1974], based on the Takeda model without hardening; see Miranda and Ruiz-García [2000, 2002]. The CSM-FEMA440 uses innovative methods to compute the effective period, the effective damping, and the demand spectrum reduction factors. It also introduces a new concept of modified acceleration-displacement response spectrum (MADRS) [ATC, 2005].

2.4. MDOF Final Results

The target displacement of the MDOF system is obtained from the equivalent SDOF target displacement previously computed, using the corresponding transformation factor.

The final results of the MPA are obtained combining the results of each pushover analysis corresponding to each mode of vibration. In order to take into account the torsional effects, the extended N2 method multiplies the obtained results by correction factors computed from the ratio between a linear response spectrum analysis (RSA) and a pushover analysis [Fajfar *et al.*, 2005].

3. Case Studies

The first building selected for this work is a real existing Turkish reinforced concrete building, with 5 stories. It experienced the 1999 Golcuk earthquake without any damage. The building was designed according to the 1975 Seismic Code of Turkey.

The building is asymmetric along the X direction (Fig. 1a), and all of the floors have the same height of 2.8 m (Fig. 1b). The building presents beams framing into beams leading to potentially weak connections in the structure. There are also walls and elongated columns, as presented in Fig. 1a.

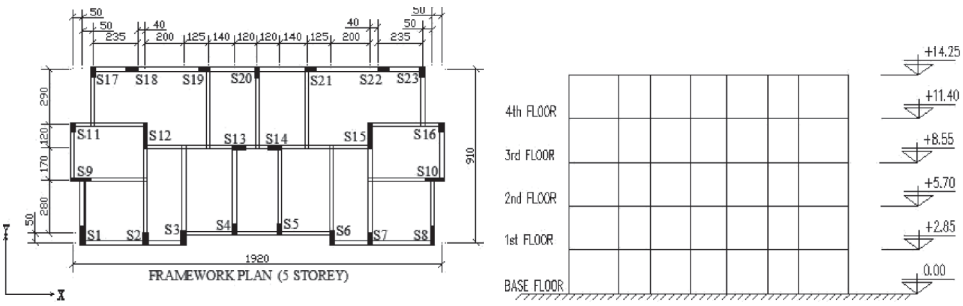

(a) (b)

FIGURE 1 (a) Plan view (cm); (b) lateral view (m).

The columns geometrical and reinforcement features are kept constant along the height of the building. The beam sections are mainly 0.20×0.50 m^2, except the two located in the center of the building that are 0.20×0.60 m^2. The stirrups have 20 cm spacing both for beams and columns. In columns, the stirrups have a diameter of 8 mm with 20 cm spacing, constant along the height. The slabs are 0.10 m and 0.12 m thick. For more details on the building's characteristics, see Vuran *et al.* [2008].

The mass of each story is considered to be 263 ton, except in the last story where the mass is 150 ton.

The second case study is a real existing Turkish reinforced concrete building with eight stories. The building was also designed according to the 1975 Seismic Code of Turkey. It is a plan irregular structure since it is asymmetric along the X and Y directions; see Fig. 2a. The first story height amounts to 5.00 m and the other floors have the same 2.70 m height; see Fig. 2b. There are beams framing into beams leading to possible weak connections in the structure. The structural vertical elements are walls and elongated columns, as presented in Fig. 2a, with the higher dimension always along the Y direction. For this reason, the structure will be more stiff and resistant along this direction.

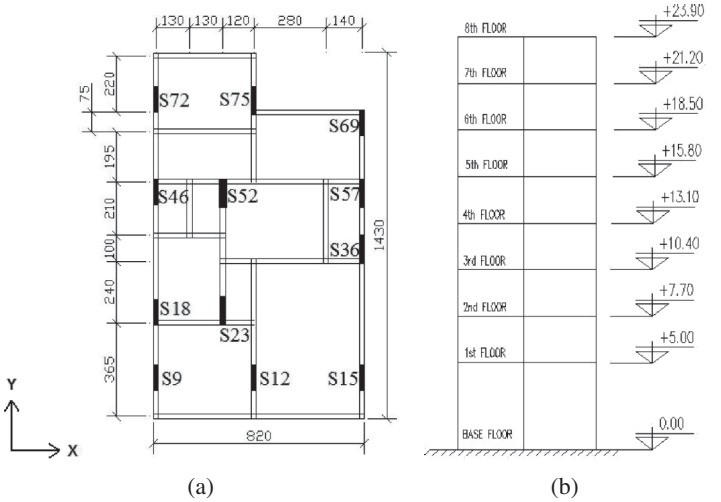

(a) (b)

FIGURE 2 (a) Plan view (cm); (b) lateral view (m).

The column sections and reinforcement keep the same geometrical features along the height of the building, except the column S52 that varies from 1.1×0.3 m^2 (on the first floor) to 0.8×0.3 m^2 (on the last floor). The height of this section is reduced by 0.1 m at every 2 stories. In columns, the stirrups are ø8 with 20 cm spacing, constant along the height.

The beam sections are mainly 0.20×0.50 m^2, except the two located in the center of the building along the X direction that are 0.30×0.50 m^2 and 0.25×0.50 m^2, respectively. The slabs are 0.12 m thick.

The mass in the first story of the 8-story building is 73 ton, 65 ton in the upper stories, and 56 ton in the last story.

4. Modeling Issues

The structural analysis software used in this study was SeismoStruct [SeismoSoft, 2006], a fibre-based structural analysis program.

The 3D buildings were represented with space frame models assuming the centerlines dimensions. Distributed material inelasticity was considered through the use of displacement-based elements while the geometric nonlinearity was taken into account utilizing corotational formulation. Each element was discretized into five sub-elements with two integration Gauss points each. Fiberized cross sections were defined at integration points. Each fiber was assigned to the respective material constitutive relationship, representing the sectional details like the cover, core concrete, and longitudinal reinforcements. The stress-strain state of the section in the beam-column elements is obtained by integrating the nonlinear uniaxial stress-strain response of the fibers using mid-point rule. The response of the elements is determined using the Gauss-Lengendre integration scheme considering the section responses at integration points.

Hysteretic damping was implicitly included in the nonlinear fiber model formulation of the inelastic frame elements. In order to take into account possible non hysteretic sources of damping, it was considered a 5% tangent stiffness-proportional damping.

The concrete was represented by a uniaxial model that follows the constitutive relationship proposed by Mander *et al.* [1988] and the cyclic rules proposed by Martinez-Rueda and Elnashai [1997]. The confinement effects provided by the lateral transverse reinforcement are incorporated through the rules proposed by Mander *et al.* [1988], whereby constant confining pressure is assumed throughout the entire stress-strain range. An average compressive strength of 16.7 MPa was considered.

The constitutive model used for the steel was the one proposed by Menegotto and Pinto [1973], coupled with the isotropic hardening rules proposed by Filippou *et al.* [1983]. Average yield strength of 371 MPa was assumed.

Since there were no available data about the material properties of the analyzed buildings, the average values used were based on extensive laboratory tests on core samples collected from and around Istanbul [Bal *et al.*, 2008], where the buildings are located. These values represent the material properties of the existing building stock in the northern Marmara region.

The rigid diaphragm effect was modelled using the Nodal Constraints Rigid Diaphragm with Penalty Functions option. The penalty function exponent used was 10^7.

In the five-story building, four controlled elements were chosen to evaluate the NSPs' performance: columns S1, S23, S13, and S14 (see Fig. 1a).

In the eight-story building, six controlled elements were monitorized: columns S9, S69, S15, S72, S23, and S52 (Fig. 2a).

5. Seismic Assessment Features

In the nonlinear dynamic analyses, three bi-directional semi-artificial ground motion records were considered. They were obtained from three real records (Table 1), taken from the PEER's database website [PEER, 2009].

The records were fitted to the Eurocode8 [CEN, 2004] elastic design spectrum (with the Turkish code features – Type 1, soil A) using the software RSPMatch2005 [Hancock *et al.*, 2006].

The ground motions were scaled for intensity levels of peak ground accelerations of 0.1, 0.2, 0.4, 0.6, and 0.8 g for the 5-story building and for 0.1, 0.2, and 0.4 g for the 8-story building.

Each bi-directional record was applied twice in each building, changing the direction of the components and resulting in 6 time-history analyses for each intensity level for each building, which means 30 analyses for the 5-story building and 18 analyses for the 8-story building. Each time-history analysis was very time consuming due to the large memory size of the numerical models. This is the reason why a larger number of records was not considered. In order to assess if the number of records used was representative, the buildings were tested for one intensity level, using three more records. The differences of the results obtained were not considerable, so the nonlinear dynamic analyses performed herein seems to get an adequate overview on the buildings' behavior.

The main concern about using scaling accelerograms (IDA) lies with the fact that low intensity records are not representative of high intensity ones. It is important to know if the median results of a certain damage measure (DM), which are obtained from records scaled for an intensity measure (IM) such as the peak ground acceleration (PGA), estimate in an accurate fashion the median DM of a set of unscaled records with the same IM. Several questions have been discussed about this topic [Shome and Cornell, 1998, 1999]. In Vamvatsikos and Cornell [2002] it is said that IDA leads to accurate estimations of DM if the IM has been chosen such that the regression of DM jointly on IM, magnitude (M), and distance (R) is independent of M and R in the range under analysis.

The IDA is much more practical than a cloud analysis (i.e., selecting several acceleration records that represent various intensity levels from multiple events and running the analyses with these records), because a smaller number of records need to be selected. For the purpose of this article, the use of semi-artificial ground motions scaled for different levels of seismic intensity seems to be an optimal solution taking into account the number of analyses performed and the time consumed.

Two types of pushover analyses were carried out: the so-called conventional force pushover and the Displacement-based Adaptive (DAP) pushover algorithm [Antoniou and Pinho, 2004]. In both cases, the force/displacement loads were applied independently in the two horizontal positive/negative directions. The target displacement was computed for each of the resulting eight loading cases, choosing the larger value in each direction.

TABLE 1 Records used in this study

Earthquake name	Year	ClstD (km)	Earthquake magnitude	Site classification Campbell's geocode
Tabas, Iran	1978	13.94	7.35	Firm Rock
Whittier Narrows-01	1987	40.61	5.99	Very Firm Soil
Northridge-01	1994	37.19	6.69	Firm Rock

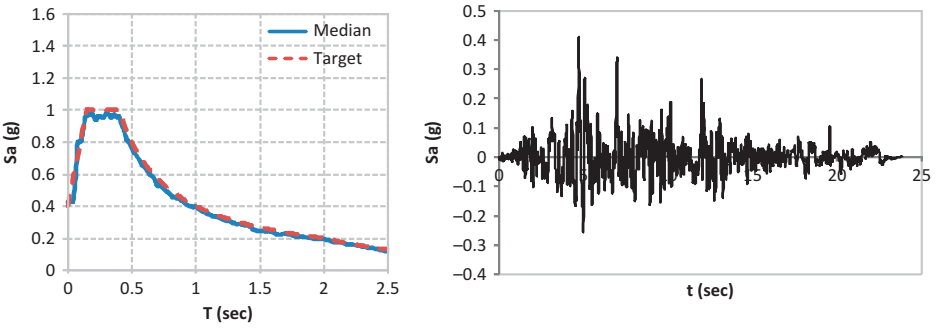

FIGURE 3 (a) Response spectrum, 0.4 g; (b) record Tabas, Iran, component 2 (color figure available online).

For each intensity level, the median spectrum used in the NSPs was obtained from the six response spectra compatible with all the six components of the three bi-directional records. The median and Eurocode 8's target response spectra for 0.4 g are represented in Fig. 3a. One of the components of one of the real records considered is plotted in Fig. 3b.

The results in terms of top displacements, base shear, lateral displacement profiles, interstory drifts, chord rotations, and top rotations in the two directions were calculated and compared for all seismic intensity levels, and for all nonlinear static procedures and nonlinear dynamic analyses. The damage limitation according to the Eurocode 8 was also checked through all the seismic intensities for the two buildings.

6. Numerical Study Results

In this chapter, the results of the five- and eight-story buildings are presented in terms of lateral displacement profiles, top displacements and base ratios, interstory drifts, chord rotations, and normalized top displacements, for different levels of seismic intensities. The discussion will be focused mainly in the inelastic range, because the NSPs were developed to evaluate the structural response at this stage.

6.1. Five-Story Building

A modal proportional load pattern, a uniform load pattern, and a DAP procedure were applied in the X and Y directions, in both positive and negative senses. The pushover curves obtained are plotted in Fig. 4, against the nonlinear dynamic analysis median results (represented as TH).

The pushover curves obtained from a uniform load pattern and the DAP analysis are almost coincidental in the X direction for both positive and negative senses. In the Y direction, these curves are equal in the elastic stage, but in the inelastic range the DAP curve tends to present higher values of base shear than the uniform load pattern curve for the same level of top displacement. The curve obtained with a modal proportional load pattern presents lower values of base shear than the other curves for the same top displacement.

From Fig. 4 one can conclude that, for the elastic range of 0.1 and 0.2 g, and for medium levels of inelasticity, 0.4 g, the time-history median results perfectly match

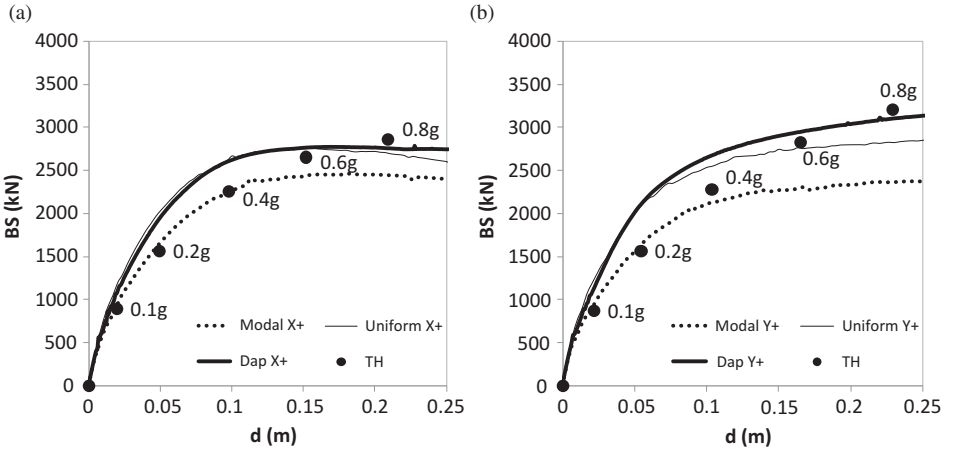

FIGURE 4 Five-story building capacity curves: (a) X; (b) Y.

the pushover curves obtained from a modal proportional load pattern in both X and Y directions, with both positive and negative senses.

For higher levels of inelasticity, 0.6 and 0.8 g, the nonlinear dynamic median results match the pushover curves obtained from the uniform load pattern and from DAP analysis in both X and Y directions, for both positive and negative senses. The pushover curves show that the building has more strength in the Y direction.

Ratios of the values obtained with the analyzed nonlinear static procedures and the corresponding median estimates coming from the nonlinear dynamic analysis (Eq. (6.1)) are computed. As it was mentioned in Sec. 2, the NSPs must never lead to underestimated results, therefore these ratios should always be higher than 1. Ideally, one would desire such ratios to tend to unity, which means the NSPs would perfectly match the time-history median results.

$$\textit{Top Displacement ratio} = \frac{\textit{NSP's top displacement}}{\textit{Time history median top displacement}} \tag{6.1}$$

These ratios, in terms of top displacements in the center of mass, corresponding to the target displacements, and in other columns of the five-story building, are plotted in Figs. 5 and 6, where TH represents the time-history results. In each figure and for each level of intensity, a line representing the dispersion of the time-history results ([mean – standard deviation, mean + standard deviation]) is also plotted.

In the inelastic range in the X direction, all the methods lead to the same conservative predictions. In the Y direction, the ACSM perfectly matches the time-history and the other methods lead to the same and conservative predictions. From the plots, one can confirm that the dispersion of the time-history results is not very high, leading to the conclusion that the number and type of records chosen for this study proved to be enough to get reliable results in the five-story building. One can also observe that, as far as top displacement ratios are concerned, the ACSM and CSM-FEMA440 lead, in general, to results close to the time-history median and always within the range [mean – standard deviation, mean + standard deviation]. This fact proves their good performance on estimating such measure. The extended N2 and the MPA are generally close to the upper bound of this range, mean + standard deviation.

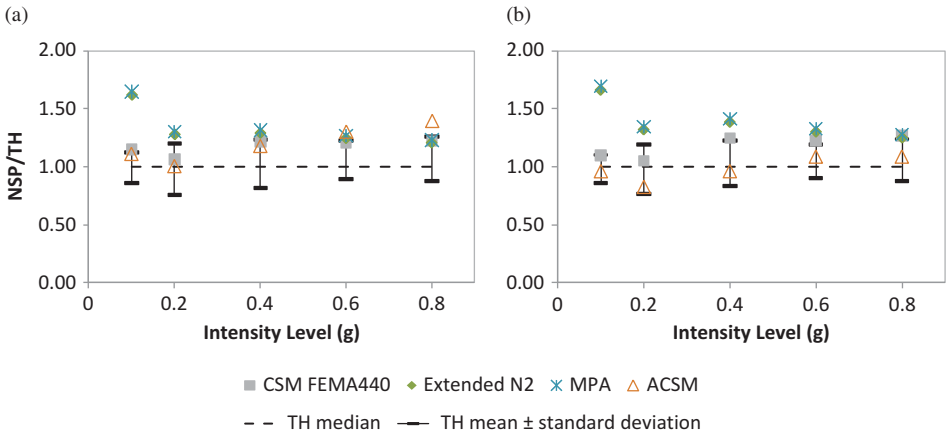

FIGURE 5 Top displacement ratios in the center of mass: (a) X direction; (b) Y direction (color figure available online).

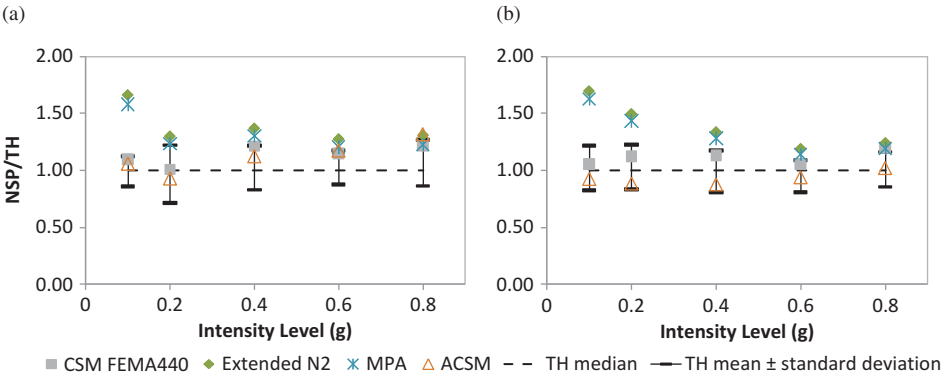

FIGURE 6 Top displacement ratios: (a) column S1 X direction; (b) S23 Y direction (color figure available online).

The comparison of the different NSPs and the nonlinear dynamic results in terms of lateral displacement profiles, interstory drifts and chord rotations are plotted in Figs. 7, 8, and 9.

The results obtained from the parametric study developed for the five-story building show that the nonlinear static procedures generally lead to conservative results. In terms of lateral displacement profiles (Figs. 7 and 8a), interstory drifts (Figs. 8b and 9a), and chord rotations (Fig. 9b) in the X direction, the asymmetric direction of the building, one can clearly conclude that for medium levels of inelasticity:

- The results computed with the CSM-FEMA440 and the ACSM match the nonlinear time-history analysis.
- Both extended N2 and MPA procedures generally lead to conservative estimations.

For higher levels of inelasticity, all NSPs tend to reproduce conservatively the response of the building in the X direction.

In the Y direction, the symmetric direction of the building, the evaluation of the same measures for medium levels of inelasticity, shows that:

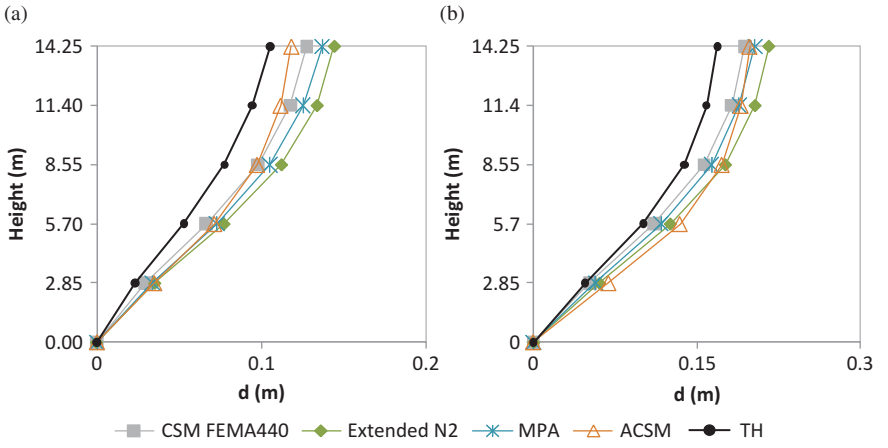

FIGURE 7 Lateral displacement profiles: (a) X 0.4 g column S1; (b) X 0.6 g column S1 (color figure available online).

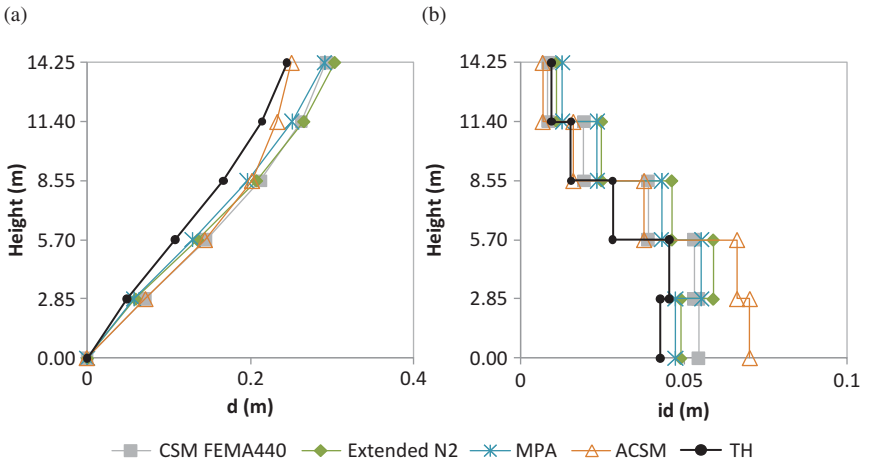

FIGURE 8 (a) Lateral displacement profiles Y 0.8 g column S23; (b) Interstory drifts X 0.6 g column S23 (color figure available online).

- the CSM-FEMA440 and the ACSM lead to results very close to the nonlinear dynamic analysis;
- the extended N2 and the MPA methods lead to conservative results.

For higher levels of inelasticity in the Y direction:

- the results computed with the ACSM match the time-history analysis;
- the CSM-FEMA440, the extended N2, and the MPA lead to similar and conservative results.

As it was observed the ACSM matched in good fashion the interstory drifts and chord rotation profiles, although it led to slightly underestimated results in the upper floors through all the seismic intensities tested.

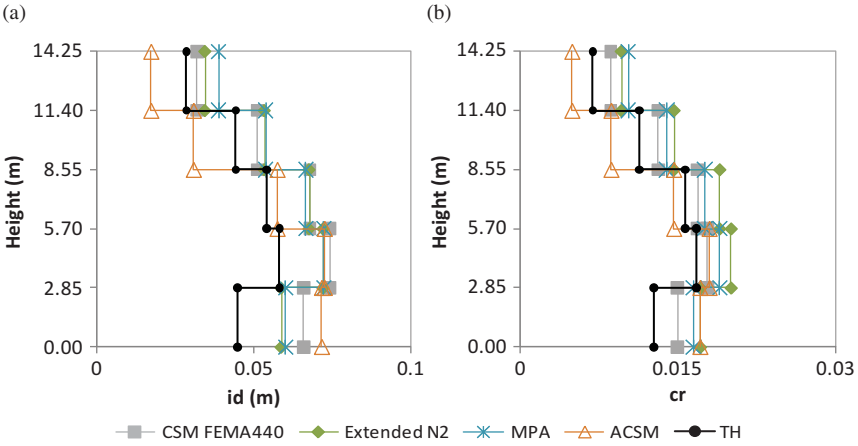

FIGURE 9 (a) Interstory drifts Y 0.8 g column S14; (b) Chord rotations Y 0.6 g column S1 (color figure available online).

In order to study the torsional behavior of plan asymmetric buildings one should analyze the trend of normalized top displacements (Fajfar *et al.*, 2005). This measure is obtained by normalizing the edge displacement values with respect to those of the center of mass. The torsional response in the time-history is taken from the step of the analysis correspondent to the maximum top displacement (in absolute value) in the center of mass. These measures are plotted in Figs. 10 and 11, in the X direction for increasing seismic intensities.

In terms of normalized top displacements, the extended N2 method was the one that better reproduced the torsional motion of the building in the X direction (the asymmetric direction of the structure). In fact, the method perfectly captures the torsional amplification on the flexible edge of the building, column S1, for 0.2 and 0.6 g. For 0.4 and 0.8 g, it slightly overestimated the response. The extended N2 method led to conservative results on the stiff side of the building, column S23, through all the seismic intensities, because it does not consider any positive effect due to torsion.

The CSM-FEMA440 and MPA led to the same results of normalized top displacements. They perfectly reproduced the time-history on the flexible side for 0.4 and 0.8 g, but they

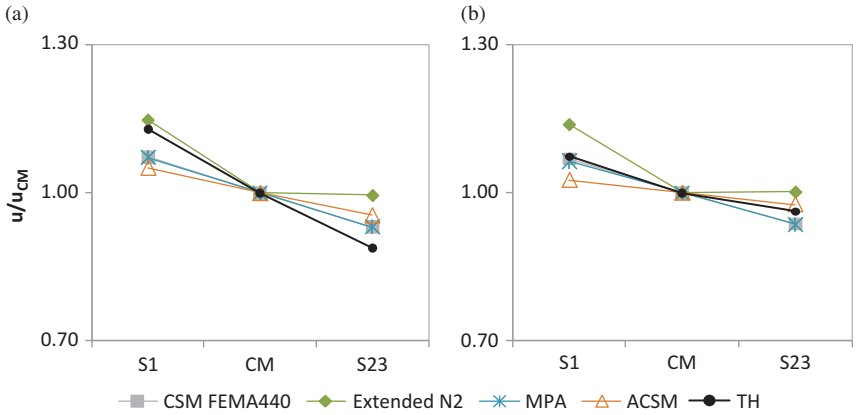

FIGURE 10 Normalized top displacements X direction: (a) 0.2 g; (b) 0.4 g (color figure available online).

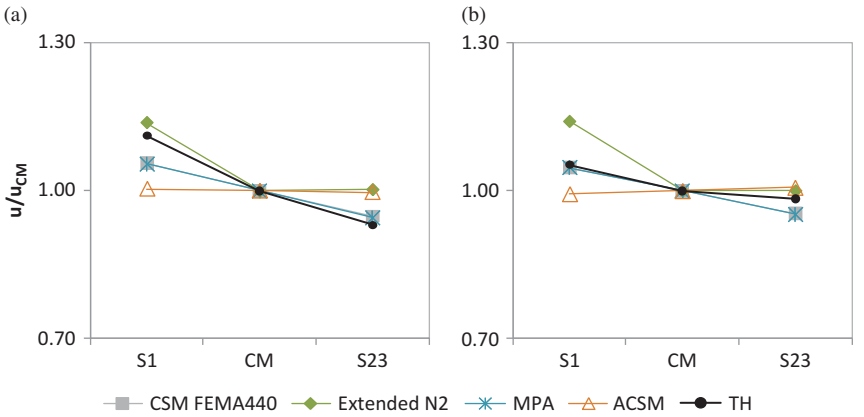

FIGURE 11 Normalized top displacements X direction: (a) 0.6 g; (b) 0.8 g (color figure available online).

underestimated the results for 0.2 and 0.6 g. The methods slightly overestimate the response on the stiff side for 0.2 and 0.6 g, but they led to non conservative estimations for 0.4 and 0.8 g.

The ACSM generally underestimated the results on the flexible side through all the seismic intensities tested. On the other hand, the procedure led to overestimated results on the stiff edge for 0.2 and 0.6g. For 0.4 and 0.8 g, the method reproduced, in a very good fashion, the response on this side of the building.

The CSM-FEMA440, MPA, and ACSM always predicted the torsional motion of the building in a linear way from one side of the building to the other. The extended N2 method does not estimate this motion linearly because no de-amplification due to torsion is taken into account in its theoretical background.

One can also notice a flattening on the normalized top displacements curves as the seismic intensity increases. This fact confirms the idea that the torsional effects are higher for lower levels of seismic intensity, reducing its effect when the maximum ground accelerations increase.

6.2. Eight-Story Building

In Fig. 12, the pushover curves obtained for the eight-story building are plotted against the time-history median results. One can observe that in the X direction, Fig. 12a, both DAP and conventional pushover, with a modal proportional and uniform load patterns, lead to the same results. They perfectly match the nonlinear dynamic median results for all intensities tested. In the Y direction, Fig. 12b, the three pushover curves lead to the same results in the elastic stage, perfectly matching the time-history. In the inelastic stage, the DAP curve leads to higher base shear values among all the curves, for the same level of displacement.

Also from Fig. 12, one can conclude that the building presents a clearly unbalanced stiffness distribution between the two directions. In fact, the Y direction is much more stiff and resistant than the X direction. Figure 12b also shows that the building remains elastic in the Y direction through all the seismic intensities analyzed.

The ratios of top displacements and of the base shear, for all the seismic intensities studied, are plotted in Figs. 13 and 14. The dispersion of the time-history results in terms of top displacements is also plotted in the figures, as was done for the five-story building.

From Figs. 13a and 14, one can observe that the ACSM and CSM-FEMA440 are the methods that get closer to the time-history results in terms of top displacements through

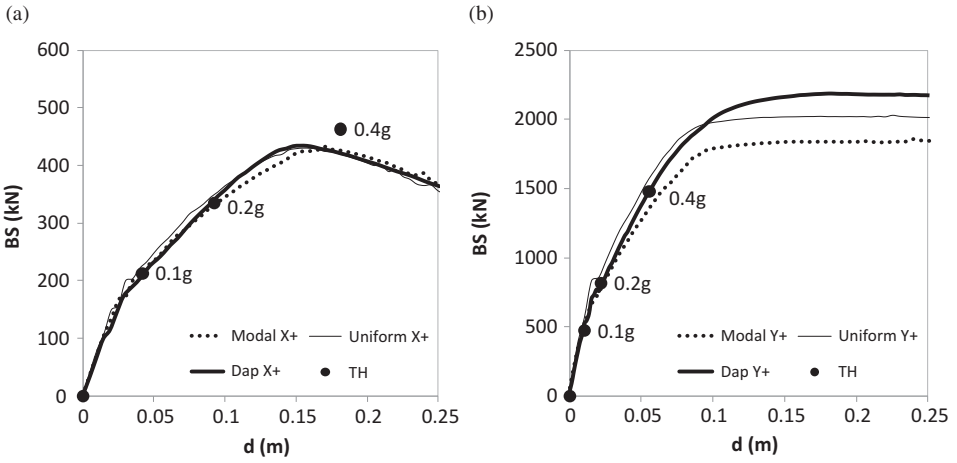

FIGURE 12 Eight-story building capacity curves: (a) X; (b) Y.

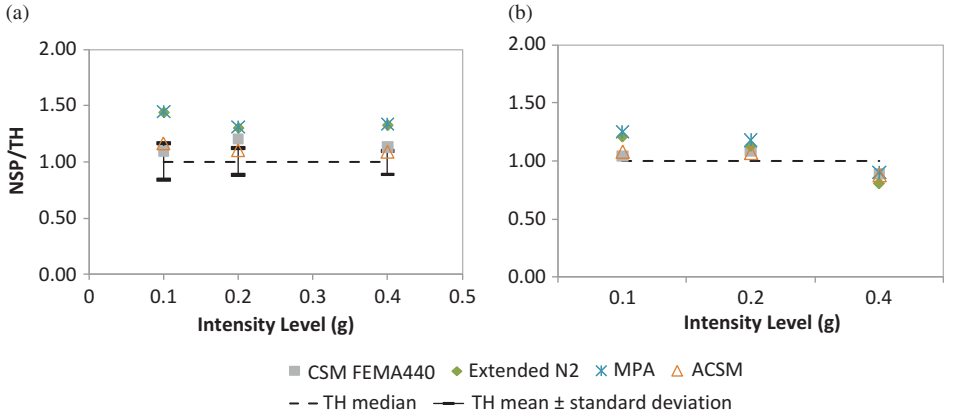

FIGURE 13 (a) Top displacements ratios in the center of mass X direction; (b) base shear ratios X direction (color figure available online).

all the seismic intensities. The extended N2 and the MPA generally lead to conservative results.

As far as base shear ratios are concerned (see Fig. 13b), once again the ACSM and CSM-FEMA440 lead to almost perfect predictions for 0.1 and 0.2 g, while the other two methods slightly overestimated the response. For 0.4 g, corresponding to a high level of inelasticity, all the NSPs lead to the same results but slightly non conservative. From the figures representing the top displacement ratios, it is evident that the distribution of the time-history results has a relatively small dispersion. This confirms that the number and type of records used in this study seem to be enough to get reliable results in the eight-story building. One can also observe that the ACSM and CSM-FEMA440 lead to top displacement ratios very close to the upper bound of the time-history distribution range – mean + standard deviation – while the other two methods lead to values slightly above this range.

The results in terms of lateral displacement profiles, interstory drifts, and chord rotations for the eight-story building are plotted in Figs. 15, 16, and 17. From the plots it is

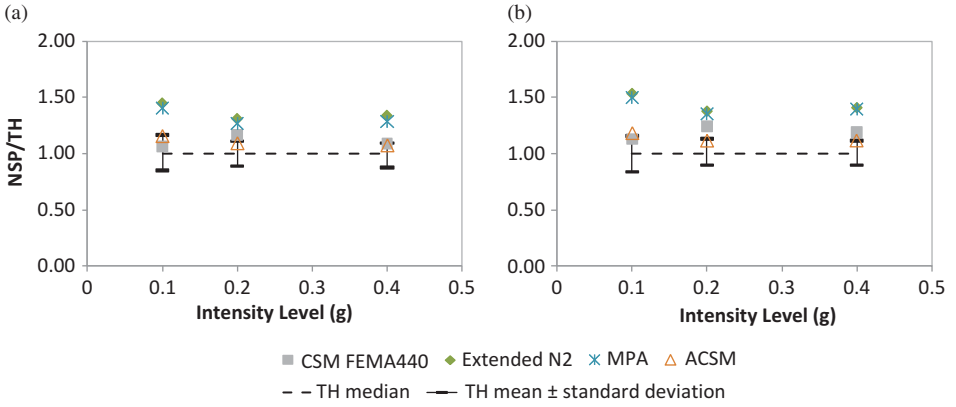

FIGURE 14 Top displacements ratios in the X direction: (a) column S9; (b) column S69 (color figure available online).

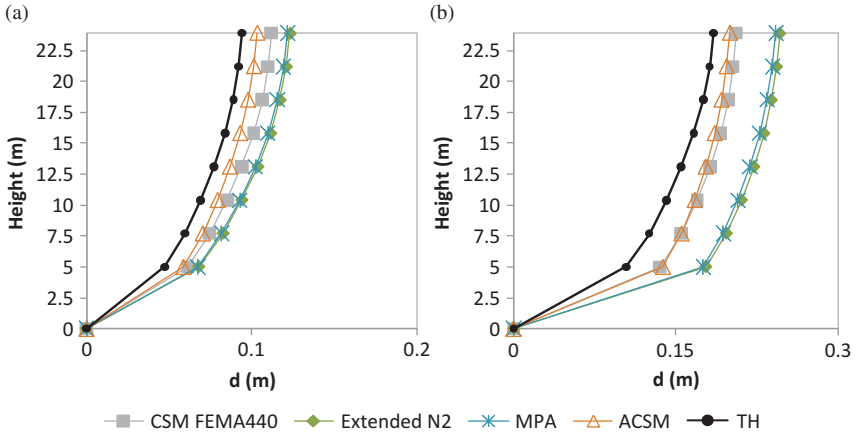

FIGURE 15 Lateral displacement profiles: (a) X 0.2 g column S23; (b) X 0.4 g column S23 (color figure available online).

clear that the building presents a soft-story mechanism on the first floor along the X direction, collapsing due to this local mechanism for 0.4 g. In fact, the interstory drifts and chord rotations are much higher on the first story than in the upper floors. This trend is observed through all the seismic intensities tested. The ACSM and CSM-FEMA440 are the methods that better reproduce this phenomenon. The extended N2 and the MPA slightly overestimate this mechanism. In fact, the ACSM is able to predict correctly the soft-story mechanism because it uses the DAP method where the properties of the damaged structures are updated and fed into the model in each analysis step. The soft-story mechanism on the first floor can be explained by the considerable difference between the heights of the first and the second floors, inducing a considerable difference on the stiffness between these two stories. In fact, the first story height amounts to 5 m and the upper floors to 2.70 m, therefore the first floor is more flexible than the upper ones, leading to a local mechanism. This phenomenon also explains why the pushover curves of the building present less strength and stiffness in the X direction, as illustrated in Fig. 12. These characteristics lead

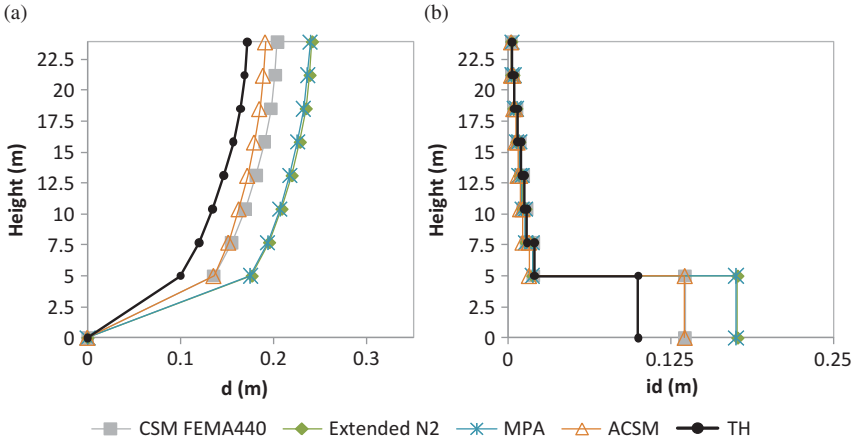

FIGURE 16 (a) Lateral displacement profiles X 0.4 g column S69; (b) interstory drifts X 0.4 g column S69 (color figure available online).

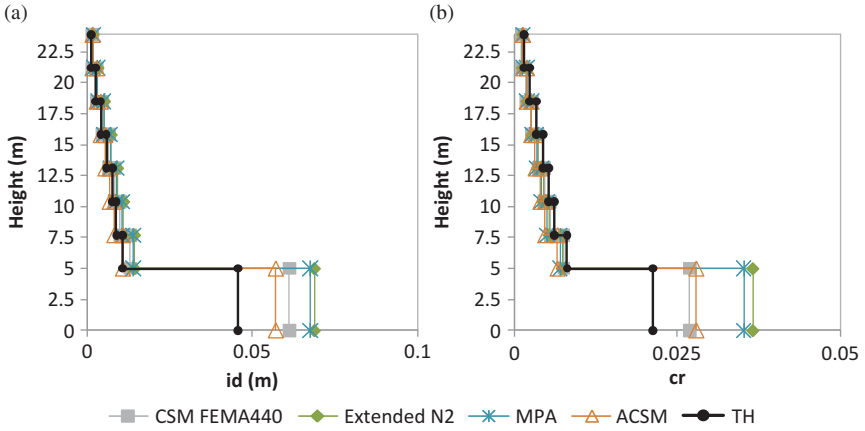

FIGURE 17 (a) Interstory drifts X 0.2 g column S72; (b) chord rotations X 0.4 g column S9 (color figure available online).

the building to behave inelastically only in the X direction, keeping the response elastic in the Y direction.

As the intensity increases and the structure goes through higher levels of inelasticity, all the methods seem to overestimate the lateral displacement profiles. Although the ACSM and CSM-FEMA440 are the methods that lead to results closer to the nonlinear dynamic analysis, this trend is clear mainly on the first floor where the soft-story mechanism is quite well reproduced by these two methods.

In terms of interstory drifts and chord rotations (see Figs. 16b and 17), one can observe that for the upper stories, all the NSPs lead to the same results, very close to the time-history. The normalized top displacements in both X and Y directions are plotted in Fig. 18, for increasing seismic intensities.

Figure 18a, shows that the extended N2 method could perfectly capture the torsional amplification on column S9 in the X direction. On the opposite edge, the method overestimates the seismic response because it does not consider any de-amplification due to torsion.

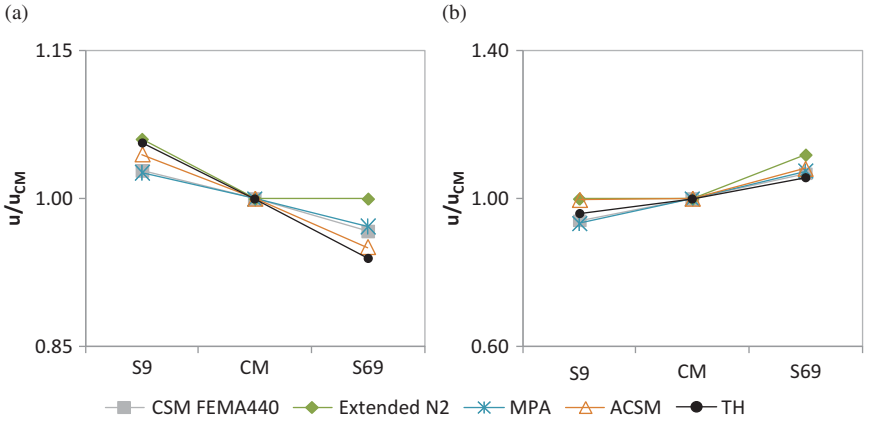

FIGURE 18 Normalized top displacements: (a) X 0.1 g; (b) Y 0.4 g (color figure available online).

The CSM-FEMA440 and MPA lead to similar results in the X direction. They estimate linearly the response from one side of the building to the other, underestimating the torsional amplification on column S9 and overestimating on column S69. The ACSM could perfectly capture the torsional de-amplification on column S69, but it slightly underestimated the amplification on the opposite edge.

In the Y direction (see Fig. 18b), it is clear that all the NSPs predict, in a very good way, the torsional amplification on column S69. On the opposite edge, the extended N2 and the ACSM slightly overestimate the response while the other two methods slightly underestimate the torsional de-amplification.

It is also evident from Fig. 18 that the torsional effect decreases as the seismic intensity increases. This can be concluded by the flattening of the normalized top displacements from 0.1–0.4 g.

It is interesting to note that all pushover analysis can positively reproduce the specific characteristics of the building's structural response through all the seismic intensities tested, namely:

- The unbalanced stiffness distribution between the two directions:
  - the Y direction is much more stiff than the X direction;
  - the response of the building remains elastic in the Y direction through all the intensity levels analyzed;
- The collapse of the building due to a soft-story mechanism in the first floor along the X direction.

6.3. Damage Limitation Control According to Eurocode 8

In this section, the damage limitation requirement according to the Eurocode 8 is evaluated. This verification is done in terms of interstory drift limitation. Since the buildings under analysis have non structural elements of brittle materials attached to the structure, the interstory drift limit is defined in Eq. (6.2):

$$d_r \nu \leq 0{,}005\, h, \tag{6.2}$$

where
d_r is the design interstory drift;
h is the story height;
ν is the reduction factor, which takes into account the lower return period of the seismic action associated with the damage limitation requirement.

The value of ν depends on the importance class of the building. Since the case studies under analysis belong to an Importance Class II, the value ascribed to ν is 0.5.

The elements analyzed within this damage limitation verification were columns S1, S23, S13, and S14 for the five-story building and columns S9, S69, S15, S72, S23, and S52 for the eight-story building. These columns were verified in all stories, in both X and Y directions, through all the seismic intensities tested. The number of columns evaluated in each building is sufficient so one can understand the trend of how accurately each NSP perform in verifying the exceedance of the damage limitation criterion.

The last column of Tables 2–5 present the number of elements that exceeded the interstory drift damage limitation defined according to EC8, resulting from the time-history analysis. The other columns give an insight of how many of these exceedances were captured by each NSP. These comparisons are made for all seismic intensities tested, in both X and Y directions, for the two buildings analyzed.

From Tables 2 and 3, one can conclude that in the five-story building the time-history results indicate no exceeding elements in the elastic stage, 0.1 and 0.2 g. For lower levels of inelasticity, 0.4 g, the number of exceeding elements is very small, and once again all NSPs could generally capture this behavior, except the ACSM in the Y direction. In the inelastic stage, 0.6 and 0.8 g, there is a big increase of exceeding elements. For 0.6 g, all NSPs could reproduce the time-history results, except the ACSM in the Y direction where it slightly underestimated the response. For very high levels of inelasticity, 0.8 g, all the NSPs tend

TABLE 2 Five-story building: Interstory drifts damage limitation EC8 - X direction

	CSM FEMA440	Extended N2	MPA	ACSM	Time-history
0.1 g	0	0	0	0	0
0.2 g	0	0	0	0	0
0.4 g	1	1	1	1	1
0.6 g	11	11	11	11	11
0.8 g	12	13	13	12	16

TABLE 3 Five-story building: Interstory drifts damage limitation EC8 - Y direction

	CSM FEMA440	Extended N2	MPA	ACSM	Time-history
0.1 g	0	0	0	0	0
0.2 g	0	0	0	0	0
0.4 g	2	2	2	0	2
0.6 g	14	14	14	12	14
0.8 g	19	19	19	16	19

TABLE 4 Eight-story building: Interstory drifts damage limitation EC8 - X direction

	CSM FEMA440	Extended N2	MPA	ACSM	Time-history
0.1 g	0	0	0	0	0
0.2 g	0	0	0	0	0
0.4 g	6	6	6	6	6

TABLE 5 Eight-story building: Interstory drifts damage limitation EC8 - Y direction

	CSM FEMA440	Extended N2	MPA	ACSM	Time-history
0.1 g	0	0	0	0	0
0.2 g	0	0	0	0	0
0.4,g	0	0	0	0	0

to slightly underestimate the results obtained with the nonlinear dynamic analysis in the X direction. In the Y direction, they could capture the real response of the building, except the ACSM that underestimated it.

The ACSM usually reproduces quite well the time-history response profiles through different seismic intensities. Despite its accuracy in terms of profile shapes, the method leads sometimes to non conservative estimations when compared with the nonlinear dynamic median results. This fact is more relevant when analyzing damage limitation criteria. In fact, if the method leads to a response smaller than the damage limitation, even if it is a slightly underestimation, the element under consideration is not considered to exceed the damage criterion. This explains why the ACSM underestimates the number of damaged elements even though it reproduces in a good fashion the time-history response profiles.

From Table 4, it is clear that the eight-story building did not present any element exceeding the damage limitation criterion for 0.1 and 0.2 g in the X direction. For 0.4 g, 6 elements exceeded the limit, being well captured by all the NSPs. The results obtained by the NSPs were the same from those of time-history, through all the seismic intensities tested.

Table 5 shows that any element exceeded the damage limitation in the Y direction of the eight-story building. As was mentioned before, the building remains elastic in this direction through all the seismic intensities tested.

7. Shear Strength Verification

The two buildings herein analyzed are constituted by wall-like columns. When these kinds of structures are not properly designed, the sensitiveness to shear actions can increase. This effect is more evident on old structures where there is a lack of design and construction against brittle failures. This aspect is actually very relevant because if brittle failure occurs the structure looses ductility, and the building will be subjected to an undesirable brittle collapse.

In both buildings, some characteristic columns were analyzed in terms of shear capacity for the higher seismic intensities tested. This capacity was calculated based on ATC40 recommendations. The comparison between the maximum shear value (Vsd) obtained from

the time-history analysis in each column, for each level of intensity, and the shear capacity (Vrd) are presented in Tables 6–9, for the five- and eight-story buildings.

In each column, the shear verification was performed for the yielding regions at the column ends — plastic hinge zones — and in the near midheight region of the columns. Since the transverse reinforcement is constant along the height of the column and the shear demand is also constant at each story, the conditioning zone is the region of moderate or high ductility correspondent to the plastic hinge zone. In this case, the shear strength in the midheight region of the columns is always higher than in the plastic hinge zone. In the near midheight region of the columns (low ductility zones), the shear capacity is always higher than the shear demand for the case studies analyzed. The results presented in the tables correspond to the verification in column ends.

From Tables 6 and 7, one can observe that in the five-story building brittle failure only occurs for a seismic intensity of 0.8 g, because in column S13 the shear demand in the X direction is slightly higher than its capacity in the same direction. This was the last seismic level tested in this building, corresponding to the structural collapse. For the other seismic intensities tested in the five-story building there are no problems related with brittle failure.

From Tables 8 and 9, one can conclude that there is no brittle failure in the eight-story building for any seismic intensity tested, as the shear capacity of the analyzed columns is

TABLE 6 Five-story building: Shear vs. shear capacity - X direction (units kN)

	S1		S13		S14		S23	
Intensity level (g)	Vsd	Vrd	Vsd	Vrd	Vsd	Vrd	Vsd	Vrd
0.6 g	47	156	400	490	346	491	52	149
0.8 g	51	156	556	490	465	491	60	149

TABLE 7 Five-story building: Shear vs. shear capacity - Y direction (units kN)

	S1		S13		S14		S23	
Intensity level (g)	Vsd	Vrd	Vsd	Vrd	Vsd	Vrd	Vsd	Vrd
0.6 g	216	318	91	365	80	366	91	203
0.8 g	245	318	94	365	96	366	154	203

TABLE 8 Eight-story building: Shear vs. shear capacity - X direction (units kN)

	S15		S23		S72	
Intensity level (g)	Vsd	Vrd	Vsd	Vrd	Vsd	Vrd
0.4 g	28	176	62	224	29	177

TABLE 9 Eight-story building: Shear vs. shear capacity - Y direction (units kN)

	S15		S23		S72	
Intensity level (g)	Vsd	Vrd	Vsd	Vrd	Vsd	Vrd
0.4 g	100	343	123	422	109	345

always higher than the shear demand for 0.4 g — the higher seismic level tested in this building.

8. Discussion

The use of modified records compatible with the target response spectrum (as it was done in this article), in general lead to a small response dispersion, as can be observed in Figs. 5, 6, 13a, and 14. On the contrary, the dispersion of real records is often very high. As a consequence, it is generally accepted that the number of real records needed to get reliable results is much higher than by using modified records. Since the 3D models herein developed have a considerably large memory size, the time consuming of each nonlinear dynamic analysis is also very high. If one would use real records, the number of accelerograms will be much higher, turning unfeasible the large parametric study herein developed.

However, modified records compatible with the target spectrum lead to conservative results of the median structural responses when compared to the real records. Figure 19 shows the 5% damped target spectrum as well as the real and compatible spectra for the Tabas ground motion used. These plots refer to the component of the Tabas ground motion with the highest peak ground acceleration.

In the five-story building, the spectrum values for the periods beyond the fundamental period 0.617 s are larger for the spectrum compatible record, influencing the nonlinearity effect. For the periods less than 0.617 s, the spectrum values are amplified significantly for the spectrum compatible record, influencing the higher modes effect. The same conclusions can be drawn for the eight-story building with a fundamental period of 1.445 s.

The results obtained in this study, in terms of top displacements, lateral displacements, interstory drifts, and chord rotations, showed that the CSM-FEMA440 and ACSM were the methods that better matched the nonlinear dynamic median response profiles.

The good performance of the CSM-FEMA440 can be explained due to: its new and accurate algorithm to calculate the effective period and the effective damping; and an accurate demand spectrum reduction factor coupled with the new concept of modified acceleration-displacement response spectrum (MADRS).

The ACSM apparently managed to follow the change of response characteristics slightly better with the increase of seismic intensity, most likely because of the fact that such

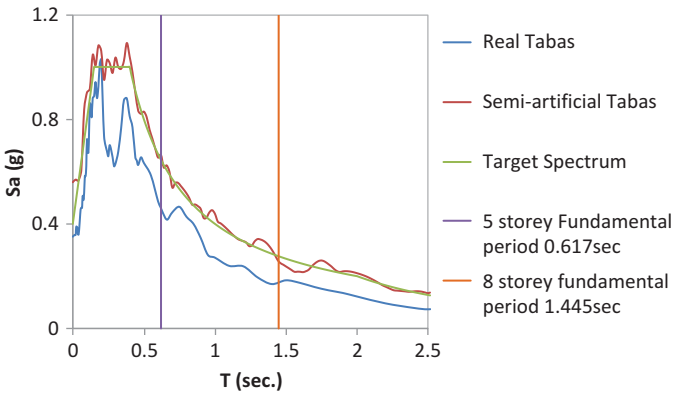

FIGURE 19 Tabas ground motion (color figure available online).

a method uses an adaptive displacement pushover (DAP) and an equivalent SDOF structural displacement built on the current deformed pattern (which can turn very useful when dealing with 3D plan asymmetric buildings). The CSM-FEMA440 and the ACSM have two essential differences: the CSM-FEMA440 uses a conventional, non adaptive, force-based pushover and the ACSM uses a displacement based adaptive pushover (DAP); the post-yield equivalent period, viscous damping ratio, and the spectrum reduction factor are obtained by using different set of equations. Both methods use reduction factors depending on the damping. The damping ratios obtained using the CSM-FEMA440 and ACSM procedures are represented in Tables 10 and 11 for the two buildings under analysis.

In the lower seismic intensities for which the buildings remain elastic, the damping ratio calculated by the methods should be equal to 5% viscous damping used in the nonlinear dynamic analysis in the elastic range.

From Tables 10 and 11, one can observe that in the five-story building in the elastic regime, 0.1 and 0.2 g, the ACSM overestimates the damping in both directions while the CSM-FEMA440 leads to damping ratios quite close to 5%. The same conclusion can be drawn in the eight-story building for an intensity of 0.1 g (elastic regime). In the inelastic range, the ACSM continues to calculate values of damping larger than the ones obtained using the CSM-FEMA440.

By using the sophisticated and powerful DAP algorithm, the ACSM could, in theory, perfectly match the time-history response. However, the equations for calculating the damping and spectral reduction factor proved to be not so accurate, since the method overestimated the damping ratios in the structures under analysis. Therefore, the final results obtained with the method were not as accurate as expected. In fact, this overestimation of the damping can explain why the ACSM leads in certain cases to underestimated results when compared with the time-history median, especially in terms of damage criteria such as interstory drifts and chord rotations.

The good results obtained with the CSM-FEMA440 are justified by the accuracy on the computation of the damping ratios and the respective spectral reduction factors. Despite using a conventional, non adaptive, force-based pushover algorithm, the CSM-FEMA440

TABLE 10 CSM-FEMA440 damping ratio (%)

	5-story		8-story
Intensity Level	X	Y	X
0.1 g	5.20	5.40	5.29
0.2 g	5.30	5.30	5.44
0.4 g	6.70	6.40	9.15
0.6 g	10.90	10.00	–

TABLE 11 ACSM damping ratio (%)

	5-story		8-story
Intensity Level	X	Y	X
0.1 g	6.51	6.79	7.28
0.2 g	7.31	6.99	7.71
0.4 g	10.24	9.29	12.34
0.6 g	13.95	11.84	–

is able to estimate a response close to the time-history because it correctly calculates the damping of the structures and the respective spectral reduction factor.

The conclusions obtained herein with these two case studies confirm the idea that in a pushover analysis all steps of a nonlinear static procedure are equally important: the pushover algorithm, the MDOF to SDOF transformation, and the calculation of the target displacement. A less accurate approach in one of the steps can justify some underestimated results.

In terms of normalized top displacements, the extended N2 method was the only method capable of reproducing the torsional motion of the buildings through increasing seismic intensities. The reason for this trend lies on the fact that such method uses correction factors based on an elastic response spectrum analysis, without considering any de-amplification of displacements due to torsion. Therefore, the method is able to capture the torsional amplification on the flexible edge of the buildings, and it generally led to conservative results on the stiff side. The other NSPs generally reproduced, in a linear way, the torsional motion from one side of the building to the other. For each intensity level in each direction, these methods were only able to capture the torsional behavior of just one side of the building, under predicting the other.

9. Conclusions

In this article, four commonly used nonlinear static procedures—the Extended N2 method, the CSM-FEMA440, the MPA, and the ACSM—were applied to real existing plan asymmetric RC buildings. The results were compared with the time-history nonlinear dynamic analyses through the use of semi-artificial ground motions. Several seismic intensities were tested in order to evaluate the NSPs performance in different inelastic structural stages.

The results obtained with these two real buildings, in terms of top displacements, lateral displacement profiles, interstory drifts and chord rotations, showed that:

- the CSM-FEMA440 and the ACSM were the methods that better matched the nonlinear dynamic analysis;
- the extended N2 method and the MPA led to close and conservative results.

In terms of normalized top displacements, the extended N2 was the method that better predicted the torsional response of the buildings through increasing seismic intensities. The other NSPs were not able to correctly reproduce the torsional behavior of the analyzed structures.

The eight-story building herein studied has a bad stiffness distribution between the two orthogonal directions, collapsing due to a soft-story mechanism on the first floor along the X direction. All NSPs were able to reproduce this local mechanism and the specific features on the seismic response of the building through all the intensity levels tested.

In terms of damage limitation control according to the EC8, all the NSPs tend to lead to similar results for the two case studies, through all the seismic intensities tested. These predictions were generally very close from those obtained from the time-history analysis.

The NSPs are used to assess new or existing buildings, therefore it is required that such methods lead to safe results. The principal aspect when evaluating a NSP is to verify that the method never leads to underestimated results, i.e., it should produce conservative estimations in respect to the time-history median results. A second aspect consists on evaluating the capability of a NSP to produce results close to the time-history median values. Considering these two aspects, the study carried out

showed that the Extended N2 method was the most powerful and complete NSP, among all the evaluated procedures, to analyze the real existing plan asymmetric buildings herein considered. In fact, the method was the only one to present always conservative results in all the analyzed measures through all the seismic intensities tested. This was evident when analyzing the normalized top displacements. The other NSPs analyzed should be improved in order to better capture the torsional motion in this kind of building.

Different typologies should be further tested in order to get definitive answers about the applicability of nonlinear static procedures on real existing buildings.

Acknowledgments

The authors would like to acknowledge the financial support of the Portuguese Foundation for Science and Technology (Ministry of Science and Technology of the Republic of Portugal) through the research project PTDC/ECM/100299/2008 and through the Ph.D. scholarship SFRH/BD/28447/2006 granted to Carlos Bhatt.

References

Antoniou, S. and Pinho, R. [2004] "Development and verification of a displacement-based adaptive pushover procedure," *Journal of Earthquake Engineering* **8**(5), 643–661.

Applied Technology Council (ATC) [2005] "Improvement of nonlinear static seismic analysis procedures," *FEMA 440 Report*, Redwood City, California.

Applied Technology Council (ATC) [1996] "Seismic evaluation and retrofit of concrete buildings," vols. 1 and 2, *Report No. ATC-40*, Redwood City, California.

Bal, I., Crowley, H., Pinho, R., and Gulay, G. [2008] "Detailed assessment of structural characteristics of Turkish RC building stock for loss assessment models," *Soil Dynamics and Earthquake Engineering* **28**, 914–932.

Bento, R., Bhatt, C., and Pinho, R. [2010] "Using nonlinear static procedures for seismic assessment of the 3D irregular SPEAR building," *Earthquakes and Structures* **1**(2), 177–195.

Casarotti, C. and Pinho, R. [2007] "An adaptive capacity spectrum method for assessment of bridges subjected to earthquake action," *Bulletin of Earthquake Engineering* **5**(3), 377–390.

CEN [2004] "Eurocode 8: Design of structures for earthquake resistance. Part 1: general rules, seismic actions and rules for buildings," EN 1998-1:2004 Comité Européen de Normalisation, Brussels, Belgium.

Chopra, A. K. and Goel, R. K. [2002] "A modal pushover analysis procedure for estimating seismic demands for buildings," *Earthquake Engineering and Structural Dynamics* **31**, 561–582.

Chopra, A. K. and Goel, R. K. [2004] "A modal pushover analysis procedure to estimate seismic demands for unsymmetric-plan buildings," *Earthquake Engineering and Structural Dynamics* **33**, 903–927.

Fajfar, P. [2000] "A nonlinear analysis method for performance-based seismic design," *Earthquake Spectra* **16**(3), 573–592.

Fajfar, P. and Fischinger, M. [1988] "N2 – A method for non-linear seismic analysis of regular buildings," *Proc. of the Ninth World Conference in Earthquake Engineering*, Tokyo-Kyoto, Japan, **5**, 111–116.

Fajfar, P., Marusic, D., Perus, I. [2005] "Torsional effects in the pushover-based seismic analysis of buildings," *Journal of Earthquake Engineering* **9**(6), 831–854.

Filippou, F. C., Popov, E. P., and Bertero, V. V. [1983] "Modeling of R/C joints under cyclic excitations," *Journal of Structural Engineering* **109**(11), 2666–2684.

Freeman, S. A. [1998] "Development and use of capacity spectrum method," *Proc. of the Sixth U.S. National Conference on Earthquake Engineering*, Seattle, USA; Paper No. 269.

Freeman, S. A., Nicoletti, J. P., and Tyrell, J. V. [1975] "Evaluation of existing buildings for seismic risk – A case study of Puget Sound Naval Shipyard, Bremerton, Washington," *Proc. of U.S. National Conference on Earthquake Engineering*, Berkley, California, pp. 113–122.

Gulkan, P. and Sozen, M. [1974] "Inelastic response of reinforced concrete structures to earthquakes motions," *ACI Journal* **71**, 604–610.

Hancock, J., Watson-Lamprey, J., Abrahamson, N. A., Bommer, J. J., Markatis, A., McCoy, E., and Mendis, R. [2006] "An improved method of matching response spectra of recorded earthquake ground motion using wavelets," *Journal of Earthquake Engineering* **10**(S1), 67–89.

Lin, Y. Y. and Chang, K. C. [2003] "A study on damping reduction factors for buildings under earthquake ground motions," *ASCE Journal of Structural Engineering* **129**(2), 206–214.

Mander, J. B., Priestley, M. J. N., and Park, R. [1988] "Theoretical stress-strain model for confined concrete," *ASCE Journal of Structural Engineering* **114**(8), 1804–1826.

Martinez-Rueda, J. E. and Elnashai, A. S. [1997] "Confined concrete model under cyclic load," *Materials and Structures* **30**(197), 139–147.

Menegotto, M. and Pinto, P. E. [1973] "Method of analysis for cyclically loaded RC plane frames including changes in geometry and non-elastic behaviour of elements under combined normal force and bending," *Symposium on the Resistance and Ultimate Deformability of Structures Acted on by Well Defined Loads*, International Association for Bridge and Structural Engineering, Zurich, Switzerland, pp. 15–22.

Miranda, E. and Ruiz-García, J. [2002] "Evaluation of approximate methods to estimate maximum inelastic displacement demands," *Earthquake Engineering and Structural Dynamics* **31**, 539–560.

Miranda, E. [2000] "Inelastic displacement ratios for structures on Brm sites," *Journal of Structural Engineering* **126**, 1150–1159.

Pacific Earthquake Engineering Research Center (PEER) [2009] "Strong ground motion database," Regents of the University of California, USA; http://peer.berkeley.edu/nga/

SeismoSoft [2006] "SeismoStruct - A computer program for static and dynamic nonlinear analysis of framed structures," available online: http://www.seismosoft.com.

Shome, N. and Cornell, C. A. [1998] "Normalization and scaling accelerograms for non-linear structural analysis," *Proc. of the Sixth U.S. National Conference on Earthquake Engineering*, Seattle, USA; Paper 243, pp. 1–12.

Shome, N. and Cornell, C. A. [1999] "Probabilistic seismic demand analysis of non-linear structures," *Report No. RMS-35*, RMS Program, Stanford University, Stanford, California, USA.

Vamvatsikos, D. and Cornell, C. A. [2002] "Incremental dynamic analysis," *Earthquake Engineering and Structural Dynamics* **31**, 491–514.

Vuran, E., Bal, Ý. E., Crowley, H., and Pinho, R. [2008] "Determination of equivalent SDOF characteristics of 3D dual structures," *Proc. of the 14th World Conference on Earthquake Engineering*, Beijing, China, Paper No: S15-031.